OPEN ACCESS
IOP Publishing

Letters

Classical and Quantum Gravity

Class. Quantum Grav. **39** (2022) 15LT01 (8pp) https://doi.org/10.1088/1361-6382/ac79f6

Letter

# Amorphous silicon nitride deposited by an $NH_3$-free plasma enhanced chemical vapor deposition method for the coatings of the next generation laser interferometer gravitational waves detector

**Dung-Sheng Tsai**[1], **Zhen-Li Huang**[2], **Wei-Chih Chang**[2] and **Shiuh Chao**[2,*]

[1] Department of Electronic Engineering, Chung Yuan Christian University, Taoyuan City 32023, Taiwan
[2] Institute of Photonics Technologies, National Tsing Hua University, Hsinchu 30013, Taiwan

E-mail: schao@ee.nthu.edu.tw

Received 15 March 2022, revised 15 June 2022
Accepted for publication 17 June 2022
Published 1 July 2022

CrossMark

**Abstract**
Cryogenic mechanical loss of the mirror coatings will result in thermal noise and limit the sensitivity of the next generation laser interferometer gravitational wave detectors operated at cryogenics. Amorphous silicon nitride (aSiN) films deposited by $NH_3$ plasma enhanced chemical vapor deposition ($NH_3$-PECVD), a coating method with potential in large area uniform coatings for the next generation detectors, were found previously to have a low cryogenic mechanical loss and without loss peaks that are common in current coatings for room temperature detectors. A positive correlation between N–H bond density and cryogenic mechanical loss in the aSiN films has been observed previously, and the existence of an N–H bond-related asymmetrical two-level system was postulated to account for the cryogenic mechanical loss. In this report, we studied an $NH_3$-free PECVD process to reduce the N–H bond concentration and hence reducing the cryogenic mechanical loss. The N–H bond density of all films deposited by the $NH_3$-free PECVD method was reduced to below the detection limit ($<10^{20}$ cm$^{-3}$). The composition of the optimized film is $SiN_{0.33}H_{0.58}$ which shows the lowest extinction coefficient ($1.21 \times 10^{-5}$ @ 1550 nm), a

*Author to whom any correspondence should be addressed.

high refractive index (2.68 @ 1550 nm), and excessively low stress (20.8 MPa), respectively. From 10 K to 120 K, cryogenic mechanical loss of the as-deposited $SiN_{0.33}H_{0.58}$ varies from $5 \times 10^{-5}$ to $8 \times 10^{-5}$ which is two to three times lower than that of the best $NH_3$-PECVD silicon nitride previously obtained. No distinctive cryogenic loss peak was found as well.

Keywords: optical coating, $NH_3$-free PECVD, silicon nitride, laser interferometer gravitational wave

(Some figures may appear in colour only in the online journal)

## 1. Introduction

Since the detection of gravitational waves (GW) signals from a binary black hole merger by the LIGO–Virgo Collaboration [1] in September 2015 [2], there has been continuing research toward cryogenic detection to reduce the thermal noise for increasing the detector sensitivity [3]. The 2.5-generation detector (i.e. KAGRA @ 20 K) and the third-generation detectors (i.e. the Einstein-telescope @ 10 K and LIGO Voyager @ 120 K) will aim to work at a cryogenic temperature [4–7] and likely at 1550 nm wavelength. However, detection at the most sensitive frequency range (≈100 Hz) will be still limited by Brownian thermal noise of the coatings [8] regardless of the current progress in reduction of the quantum noise by using squeezed light [9–11]. Thermal noise is proportional to the mechanical loss of the coating materials according to the fluctuation–dissipation theorem [12]. For mirrors of the current room temperature detectors, the coating materials are amorphous Ti:$Ta_2O_5$ (high refractive index) and $SiO_2$ (low refractive index) thin films deposited by ion-beam sputter (IBS) method [13]. However, both materials suffered from cryogenic mechanical loss peak [14–16] thus are hindered from practical applications to the coatings of the next-generation GW detectors. Furthermore, uniform coatings on the large area mirrors of the next generation detector, between 450 mm and 620 mm in diameter [17], is challenging to achieve by IBS coating method.

The chemical vapor deposition (CVD) methods are commonly used in the semiconductor integrated circuit industry to produce thin films, and uniform coatings have been demonstrated in practical applications of 18″ (450 mm) silicon wafers [18]. Notice that the coating area of the 18″ silicon wafer is close to that of the coatings planned for the Voyager mirrors [3]. Recently, Pan *et al* have reported that amorphous silicon nitride films (aSiN) deposited by an $NH_3$ plasma enhanced CVD ($NH_3$-PECVD) showed low cryogenic mechanical loss without loss peak and a high refractive index (2.28 @ 1550 nm) with an extinction coefficient of $1.51 \times 10^{-5}$ @ 1550 nm [19]. The film was demonstrated to be a potential candidate for the coatings of the next generation cryogenic mirrors with low thermal noise [20]. It was also shown that there is a positive correlation between the N–H bond concentration and the cryogenic mechanical loss in the $NH_3$-PECVD aSiN films and a phonon-assisted transition in an asymmetrical two-level-system (TLS), i.e. exchanging of positions between the $H^+$ and the electron lone pair in the amorphous network, was hypothesized to account for the observation [19]. Therefore, we are motivated in this study, to eliminate the $NH_3$ in the PECVD process, i.e. an $NH_3$-free PECVD process, for the purpose of reducing the N–H bond concentration in the aSiN films. Besides that, we have to optimize the $NH_3$-free deposition process firstly to maintain a low extinction coefficient and a high refractive index for the films. In this paper, we report the optimization of the $NH_3$-free PECVD process and the measured results on the aSiN films.

## 2. $NH_3$-free PECVD process optimization

In the PECVD process, precursor gases are fed into the reaction chamber and plasma of the free radicals of the precursors is generated by the radio frequency (RF) power [21–23]. Interactions between the free radicals occur in the plasma and on the substrate to form films. The standard precursors of the $NH_3$-PECVD process for depositing aSiN were ammonia ($NH_3$) and silane ($SiH_4$), with nitrogen ($N_2$) as the carrier gas. In our $NH_3$-free process, only $SiH_4$ and $N_2$ were used. The coating chamber of the $NH_3$-free process was an Oxford 100 PECVD cassette system. During the whole process, the substrate temperature and the total pressure were kept at 300 °C and 1 torr, respectively. We varied the $SiH_4$ and $N_2$ flow rates and the RF powers to deposit aSiN films. Since aside from the thermal noise, there is a stringent requirement on the absorption for the coatings as well, 1 ppm for the quarter-wave (QW) stack [20], therefore, we aimed to optimize the deposition process for minimum extinction coefficient firstly before looking into the cryogenic mechanical loss. A photothermal common path interferometer (PCI, SPTS Model PCI-03) [24] was used to measure the extinction coefficient at 1550 nm. The aSiN films were deposited on fused silica (Corning 7979 IR, 1 inch in diameter) for PCI measurements [25].

According to Domínguez Bucio *et al* [26], the aSiN waveguide deposited at a high $N_2/SiH_4$ flow rate ratio (980 sccm $N_2$ flow rate/1.5 sccm $SiN_4$ flow rate) and 60 W RF power showed relatively low optical propagation losses (5 dB $cm^{-1}$ @ 1550 nm). In our study, we fixed the $SiH_4$ flow rate at the minimum level allowed by the system, 5 sccm, and varied $N_2$ flow rate to obtain a large tuning range of the $N_2/SiH_4$ flow rate ratio. At first, we observed the effect of changing $N_2$ flow rate on the extinction coefficient of the aSiN films deposited at a fixed 60 W RF power. The results are shown in figure 1(a). The extinction coefficient decreases with the increasing $N_2$ flow rate from 500 sccm to 1500 sccm, showing a negative correlation between optical absorption and $N_2$ flow rate.

It was reported that N–H bond correlated with the optical absorption near 1550 nm [27], and in addition, Domínguez Bucio *et al* also reported that lower deposition RF power at a fixed $N_2/SiH_4$ flow rate ratio and pressure could produce aSiN films with lower N–H bound concentration [26]. Therefore, Domínguez Bucio's observation provided a clue for us to further reduce the optical absorption by lowering RF power. Therefore, we started from the deposition condition of a fixed flow rate of $N_2$ and $SiH_4$ at 1500 sccm and 5 sccm respectively, i.e. the right-most data point of figure 1(a), and reducing the RF power from 60 W down to 20 W. The extinction coefficients of those samples are shown in figure 1(b). As expected, the extinction coefficient of the aSiN decreases further with the decreasing RF power from 60 W to 20 W. The lowest extinction coefficient ($1.21 \times 10^{-5}$) of $NH_3$-free aSiN films was therefore obtained for the deposition condition of 20 W RF power, 1500 sccm $N_2$ flow rate, and 5 sccm $SiH_4$ flow rate.

The atomic concentrations and the chemical bond (such as N–H and Si–H) densities in the films were determined by the x-ray photoelectron spectroscopy (XPS, Thermo Fisher Scientific Theta Probe) and the Fourier transform infrared spectroscopy (FTIR, Bruker VERTEX 70 spectrometer), respectively, according to the method introduced in references [19, 28–31]. The composition of the optimized aSiN film was determined to be $SiN_{0.33}H_{0.58}$. The N–H bond density of the aSiN films shown in figures 1(a) and (b) were all below the detection limit ($<10^{20}$ $cm^{-3}$), indicating that the $NH_3$-free process is effective in reducing the N–H bonds in the film.

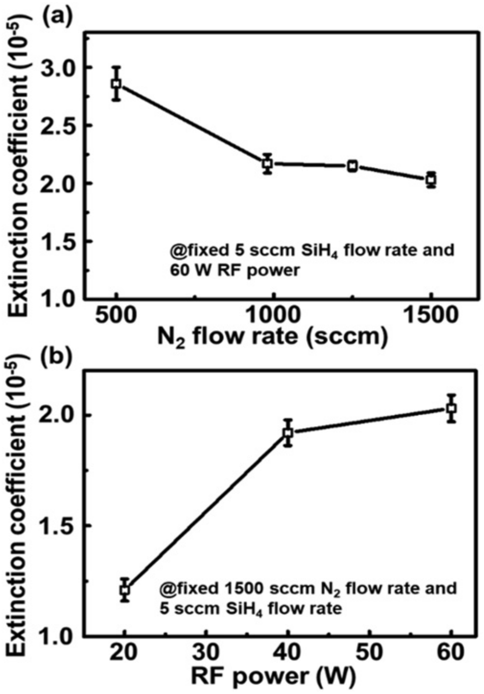


**Figure 1.** Extinction coefficient @ 1550 nm versus (a) $N_2$ flow rate and (b) different RF power. The total pressure of deposition was 1 torr.

**Table 1.** Summary of the optical and mechanical properties of the silicon nitride film.

| Composition | $n$ | $k$ ($10^{-5}$) | $E_g$ (eV) | Stress (MPa) | Y (GPa) |
|---|---|---|---|---|---|
| $SiN_{0.33}H_{0.58}$ | 2.68 ± 0.01 | 1.21 ± 0.05 | 1.9 | 20.8 ± 0.75 | 96.3 ± 1.18 |

## 3. Optical property, stress and Young's modulus measurements

The refractive index and thickness of all the $NH_3$-free aSiN samples were measured by an ellipsometer (J. A. Woollam model M2000) and the energy band gap were obtained by fitting with the Tauc–Lorentz model [32, 33]. A nano-indenter was used to measure the Young's modulus of all the $NH_3$-free aSiN films. The curvatures of the warped substrates with coatings were measured by an optical curvature meter (KLA Tencor model FLX-2320) and the stress of the films were obtained using the Stoney equation [34]. The refractive index $n$, extinction coefficient $k$, @1550 nm, energy gap $E_g$, stress and Young's modulus $Y$ of the optimized $NH_3$-free aSiN (i.e. $SiN_{0.33}H_{0.58}$) are shown in table 1.

The refractive index (2.68 @ 1550 nm) is higher than that of the previously obtained $NH_3$-aSiN films, which were from 1.78 to 2.28 increasing with decreasing N–H bond densities [19]. The $NH_3$-free aSiN is more silicon-like, i.e. Si-rich with a higher refractive index, than nitride-like of the $NH_3$-aSiN. The higher refractive index is advantageous in terms of reducing the total mechanical loss of the QW stack because the thinner physical thickness is required to achieve

QW optical thickness and less number of high-low index pairs is required to achieve a specific transmittance.

The extinction coefficient at 1550 nm, $1.21 \times 10^{-5}$, is lower than that of the previously obtained $NH_3$-aSiN films, which were from $5.47 \times 10^{-5}$ to $1.51 \times 10^{-5}$ decreasing with decreasing N–H bond densities [19]. Compared to that of the amorphous silicon films (aSi) deposited by IBS, a potential high index film for the cryogenic coating as well [25], it is lower than that of the as-deposited aSi film, $3.2 \times 10^{-4}$, and comparable to that of the lowest amorphous silicon film annealed at 400 °C, $1.22 \times 10^{-5}$. The $NH_3$-free aSiN could be incorporated into a multimaterial QW stack structure [20, 35–37] for low total absorption. The total absorption of the multimaterial QW stack is expected to be lower than 2 ppm as compared to the multimaterial QW stack for its predecessor of $NH_3$-aSiN [20].

aSiN films are generally known to show a high level of stress and the stress varies with different deposition conditions and methods [38]. Pan *et al* reported previously that there was a positive correlation between the stress of aSiN films and $NH_3/SiH_4$ flow rate ratio in the $NH_3$-PECVD process [19]. The stress of the current $NH_3$-free aSiN, essentially a zero $NH_3/SiH_4$ flow rate ratio process, is consistent with the trend of the previous observation. The stress level, 20.8 MPa in tensile, is extremely low compared to other aSiNs ever reported to our knowledge [38]. It was proposed that the replacement of the insulating Si–N structure by the conductive Si:N structure in the amorphous silicon-rich silicon nitride or amorphous nitrogen-doped silicon can reduce the stress [39]. Here, low-stress of the $NH_3$-free aSiN coatings is beneficial in preventing functional failures, such as delamination and cracking, of the coatings in the GW detector.

## 4. Cryogenic mechanical loss measurements

The cryogenic mechanical loss was measured by using the cantilever ring down method [39]. The film was coated on a silicon (110) cantilever. To balance the stress of the film, both sides of the cantilever were coated identically. The cantilever was clamped in a closed-loop cryogenic system (modified Janis SHI-4XG-15) and was excited at the resonant frequencies by an electrostatic driver. The ring down time was recorded by using a laser beam reflected from the tip of the cantilever in resonance and the signals were differentiated by a quadrant photodetector. The mechanical loss angles were then deduced from the ring-down time [40, 41]. Four modes were measured: two bending modes (669 and 1865 Hz) and two torsional modes (1284 and 3863 Hz). The temperature range of the measurement, from 10 K to 120 K, covered that for the major cryogenic detectors: 10 K for the Einstein Telescope, 20 K for KAGRA, and 120 K for Voyager.

Figures 2(a)–(d) show the cryogenic mechanical loss angles of the $NH_3$-free aSiN sample, i.e. $SiN_{0.33}H_{0.58}$ in black, and that of the lowest loss sample of the $NH_3$-aSiN, i.e. $SiN_{0.40}H_{0.79}$ in red, previously reported [19]. The loss angles for the four modes of the $NH_3$-free sample are $5.3–6.2 \times 10^{-5}$ at 10 K, $5.4–6.1 \times 10^{-5}$ at 20 K, and $7.1–8.7 \times 10^{-5}$ at 120 K, respectively, and there is no cryogenic peak. At 120 K, the proposed operating temperature of Voyager, it is obvious that the loss angles of the $NH_3$-free aSiN film are about 2–3 times lower than that of the $NH_3$-aSiN film.

Atomic densities measurements showed that $NH_3$-free aSiN is more silicon-like (i.e. silicon-rich) than the $NH_3$-aSiN. Bond densities measurements showed that decreasing of the N–H bond density was accompanied by the increase of the Si–Si and the Si–H bond densities as well as the reduction of the Si–N bond density. Variations in the atomic and bond densities provided a consistent picture with what one would expect for the difference between the $NH_3$ and the $NH_3$-free processes.

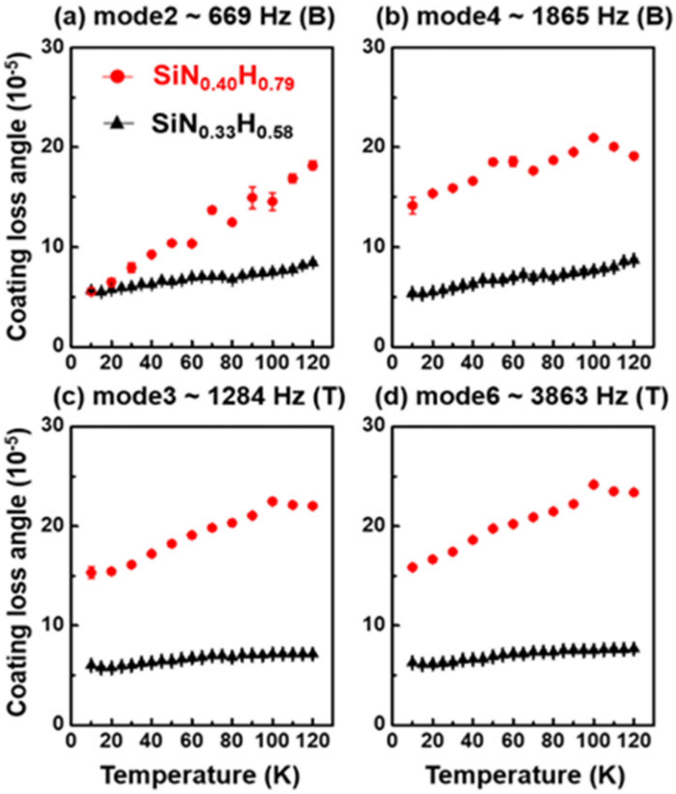


**Figure 2.** Cryogenic mechanical loss angles from 10 to 120 K for $NH_3$-free aSiN, $SiN_{0.33}H_{0.58}$ in black, and the lowest loss $NH_3$-aSiN, $SiN_{0.40}H_{0.79}$ in red from reference [19]. Four modes were measured: bending modes at (a) ∼669 and (b) ∼1865 Hz, and torsional modes at (c) ∼1284 and (d) ∼3863 Hz.

Pan *et al* proposed previously [19] that for the $NH_3$-aSiN film, the N–H correlated cryogenic mechanical loss is mainly due to the exchange positions of the electron lone pair and the $H^+$ that are associated with the N atom. The potential barrier of the transition is asymmetrical, and the transition is phonon-assisted to consume the mechanical energy. Both the single-bridging (Si–N) configuration, where there are two $H^+$ and one electron lone pair bond to the N atom, and the double-bridging (Si–N–Si) configuration, where there are one $H^+$ and one electron lone pair bond to the N atom, contribute. Based on the lower mechanical loss associated with lower N–H bond density of the $NH_3$-free aSiN, we believe that the proposed model is supported.

## 5. Conclusion

We proposed an $NH_3$-free PECVD deposition process for depositing aSiN. The N–H bond density in the film was profoundly reduced down to below the detection limit ($<10^{20}$ cm$^{-3}$), which led to a significant increase in the refractive index, decreases in extinction coefficients, stress, and cryogenic mechanical loss compared to the previously reported aSiN deposited by an $NH_3$-PECVD process. These changes are beneficial to the coatings for the next generation cryogenic laser interferometer GW detector for which low cryogenic thermal noise, low absorption, and good stability pose challenges for the mirror coatings. The results also support the proposed model of the existence of an N–H bond related asymmetrical two-level-system in the aSiN thin films, which contributes significantly to the cryogenic mechanical loss.

## Acknowledgments

DST, ZLH, WCC, and SC are financially supported by The Ministry of Science and Technology of Taiwan, The Republic of China, under Contract Nos. 106-2221-E-007-070-MY2 and 109-2112-M-033-010-MY3. The authors are grateful for the review and comments received from the Optics Working Group of the LIGO Scientific Collaboration. The LIGO document number of this paper is LIGO-P2200022.

## Data availability statement

All data that support the findings of this study are included within the article (and any supplementary files).

## ORCID iDs

Dung-Sheng Tsai https://orcid.org/0000-0003-4901-8263
Shiuh Chao https://orcid.org/0000-0003-3853-3593

## References

[1] Abbott B P *et al* 2016 *Phys. Rev. Lett.* **116** 131103
[2] Abbott B P *et al* 2016 *Phys. Rev. Lett.* **116** 061102
[3] Shapiro B *et al* 2017 *Cryogenics* **81** 83
[4] Akutsu T *et al* 2020 arXiv:2005.05574 [physics.ins-det]
[5] Science Team E T 2011 *Einstein Gravitational Wave Telescope Conceptual Design Study: ET-0106C-10* ET Technical Documentation System https://apps.et-gw.eu/tds/
[6] Adhikari R X *et al* 2020 *Class. Quantum Grav.* **37** 165003
[7] Sakakibara Y *et al* 2014 *Class. Quantum Grav.* **31** 224003
[8] Martynov D V *et al* 2016 *Phys. Rev.* D **93** 112004
[9] Abadie J *et al* (LIGO Scientifc Collaboration) 2011 *Nat. Phys.* **7** 962
[10] Aasi J *et al* (LIGO Scientific Collaboration) 2013 *Nat. Photon.* **7** 613
[11] Heurs M 2017 *Phil. Trans. R. Soc.* A **376** 20170289
[12] Callen H B and Welton T A 1951 *Phys. Rev.* **83** 34
[13] Granata M *et al* 2020 *Class. Quantum Grav.* **37** 095004
[14] Flaminio R, Franc J, Michel C, Morgado N, Pinard L and Sassolas B 2010 *Class. Quantum Grav.* **27** 084030
[15] Martin I W *et al* 2014 *Class. Quantum Grav.* **31** 035019
[16] Martin I W *et al* 2010 *Class. Quantum Grav.* **27** 225020
[17] Steinlechner J 2018 *Phil. Trans. R. Soc.* A **376** 20170282
[18] Chen M and Chang S 2016 *27th Annual SEMI Advanced Semiconductor Manufacturing Conf. (ASMC)* pp 157–9
[19] Pan H W, Kuo L C, Huang S Y, Wu M Y, Juang Y H, Lee C W, Chen H C, Wen T T and Chao S 2018 *Phys. Rev.* D **97** 022004

[20] Pan H-W, Kuo L-C, Chang L-A, Chao S, Martin I W, Steinlechner J and Fletcher M 2018 *Phys. Rev.* D **98** 102001
[21] Smith D L, Alimonda A S, Chen C C, Ready S E and Wacker B 1990 *J. Electrochem. Soc.* **137** 614
[22] Jehanathan N, Saunders M, Liu Y and Dell J 2007 *Scr. Mater.* **57** 739
[23] Knolle W R and Osenbach J W 1985 *J. Appl. Phys.* **58** 1248
[24] Alexandrovski A, Fejer M, Markosyan A and Route R 2009 *Proc. SPIE 7193 Solid State Lasers XVIII: Technology and Devices* p 71930D
[25] Birney R *et al* 2018 *Phys. Rev. Lett.* **121** 191101
[26] Domínguez Bucio T, Khokhar A Z, Lacava C, Stankovic S, Mashanovich G Z, Petropoulos P and Gardes F Y 2017 *J. Phys. D: Appl. Phys.* **50** 025106
[27] Germann R, Salemink H W M, Beyeler R, Bona G L, Horst F, Massarek I and Offrein B J 2000 *J. Electrochem. Soc.* **147** 2237
[28] Brodsky M H, Cardona M and Cuomo J J 1977 *Phys. Rev.* B **16** 3556
[29] Shanks H, Fang C J, Ley L, Cardona M, Demond F J and Kalbitzer S 1980 *Phys. Status Solidi* B **100** 43
[30] Fang C J, Gruntz K J, Ley L, Cardona M, Demond F J, Muller G and Kalbitzer S 1980 *J. Non-Cryst. Solids* **35–36** 255
[31] Morimoto A, Tsujimura Y, Kumeda M and Shimizu T 1985 *Japan J. Appl. Phys.* **24** 1394
[32] Jellison G E Jr and Modine F A 1996 *Appl. Phys. Lett.* **69** 371
[33] Nudelman S, Mitra S S and Tauc J 1969 *Optical Properties of Solids* (New York: Olenum) p 123
[34] Stoney G G 1909 *Proc. R. Soc.* A **82** 172
[35] Steinlechner J, Martin I W, Hough J, Krüger C, Rowan S and Schnabel R 2015 *Phys. Rev.* D **91** 042001
[36] Yam W, Gras S and Evans M 2015 *Phys. Rev.* D **91** 042002
[37] Craig K *et al* 2019 *Phys. Rev. Lett.* **122** 231102
[38] Hegedüs N, Balázsi K and Balázsi C 2021 *Materials* **14** 5658
[39] Temple-Boyer P, Rossi C, Saint-Etienne E and Scheid E 1998 *J. Vac. Sci. Technol.* A **16** 2003
[40] Reid S, Cagnoli G, Crooks D R M, Hough J, Murray P, Rowan S, Fejer M M, Route R and Zappe S 2006 *Phys. Lett.* A **351** 205–11
[41] Nawrodt R *et al* 2013 *Class. Quantum Grav.* **30** 115008